Acta Oceanol. Sin., 2024, Vol. 43, No. 10, P. 107–120
https://doi.org/10.1007/s13131-024-2305-z
http://www.aosocean.com
E-mail: ocean2@hyxb.org.cn

Response of phytoplankton communities to environmental changes in the Bohai Sea in late summer (2011–2020)

Yibo Wang[1, 2], Zhiliang Liu[1, 2*], Yanping Qi[3], Xiao Chen[1, 2], Yang Chen[1, 2], Du Su[1, 2], Xiaobo Yuan[1, 2], James Klippel-Cooper[4]

[1] Research Center for Marine Science, Hebei Normal University of Science and Technology, Qinhuangdao 066004, China

[2] Hebei Key Laboratory of Ocean Dynamics, Resources and Environments, Qinhuangdao 066004, China

[3] North China Sea Environmental Monitoring Center, State Oceanic Administration, Qingdao 266033, China

[4] College of Science and Engineering, Flinders University, Adelaide 5042, Australia

Received 15 November 2023; accepted 27 March 2024

Abstract

Understanding the dynamics of phytoplankton communities in coastal zones is crucial for the management and conservation of coastal ecosystems. Previous research indicated that the phytoplankton community structure and dominant taxa in the Bohai Sea (BHS) have exhibited significant shifts from the 1990s to the early 2010s in response to environmental changes, especially the change in nutrient structure. This study comprehensively investigated the variations in net-collected phytoplankton (>76 μm) community structure, diversity, and environmental factors in the BHS during the late summers of 2011–2020, aiming to understand the recent trend in phytoplankton community structure and to explore the interactions between the communities and the environment. During the study period, the nutrient status in the BHS was characterized by a decrease in dissolved inorganic nitrogen (DIN) concentration, an increase in dissolved inorganic phosphorus (DIP) concentration, and a return of the nitrogen-to-phosphorus (N/P) molar ratio (hereinafter referred to as N/P ratio) to the Redfield ratio since 2016. The eutrophication index (EI) in the BHS remained stable and was generally at a low level (<1). The Dia/Dino index fluctuated but did not show an obvious trend. Overall, the eutrophication, the imbalance in nutrient ratio, and the shift in phytoplankton community structure did not continue during the study period. The increased abundance of phytoplankton was strongly associated with elevated concentrations of DIN, as well as higher N/P and nitrogen-to-silicon (N/Si) ratios, whereas the greater diversity was strongly linked to higher concentrations of DIP. Diatoms and dinoflagellates showed significant differences in their interactions with the environment, and their relative dominance was related to water column depth and stratification intensity; their impacts on the phytoplankton community diversity were also significantly different. The variations of certain dominant species, i.e., *Skeletonema costatum*, *Paralia sulcata*, and *Tripos longipes*, exhibited strong links to the changes in nutrient structure in the BHS. The findings of this study contribute to understanding the regional environmental changes and provide insights into the adaptive strategies of coastal ecosystems in response to environmental shifts and fluctuations.

Key words: Bohai Sea, phytoplankton community, diversity, Dia/Dino index, dominant species, environmental change

Citation: Wang Yibo, Liu Zhiliang, Qi Yanping, Chen Xiao, Chen Yang, Su Du, Yuan Xiaobo, Klippel-Cooper James. 2024. Response of phytoplankton communities to environmental changes in the Bohai Sea in late summer (2011–2020). Acta Oceanologica Sinica, 43(10): 107–120, doi: 10.1007/s13131-024-2305-z

1 Introduction

Phytoplankton, accounting for nearly half of global primary production, are the foundation of the oceanic food web and key players in the global carbon cycle (Falkowski and Woodhead et al., 1992; Field et al., 1998). The variability in the abundance/biomass and taxonomic composition of phytoplankton is a critical aspect of studying global biochemical cycles and evaluating ecosystem functions (Pan et al., 2020). The abundance/biomass and distribution of phytoplankton in the natural environment are regulated by various environmental factors such as light, temperature, and nutrients (Rhee, 1982). Anthropogenic activities such as nutrient inputs from agricultural and urban runoff, along with climate change, can significantly impact phytoplankton dynamics and community structure (Raitsos et al., 2015; Richardson and Schoeman, 2004). Phytoplankton are usually spatially and temporally dynamic in biomass and community structure in coastal zones, where strong interaction between land and ocean yields highly variable physical and chemical gradients (Sun et al., 2019a; Zhu et al., 2009). A better understanding of the dynamics and variability of phytoplankton in coastal zones is crucial for the

Foundation item: The National Natural Science Foundation of China under contract No. 42206161; the Natural Science Foundation of Hebei Province under contract No. D2022407004; the Science Research Project of Hebei Education Department under contract No. QN2022167; the Open Fund Project of Hebei Key Laboratory of Ocean Dynamics, Resources and Environments under contract No. HBHY04.

*Corresponding author, E-mail: zhlliu3897@hevttc.edu.cn

effective management and conservation of marine ecosystems.

The Bohai Sea (BHS) is China's largest inland sea, covering approximately 77 000 km^2 and having an average depth of 18 m (Liu et al., 2015b; Zhai et al., 2012). The BHS consists of three bays: Liaodong Bay (LDB), Bohai Bay (BHB), and Laizhou Bay (LZB), as well as the central Bohai Sea (CB), and is connected to the Yellow Sea via the Bohai Strait (Wang et al., 2009). Approximately 40 rivers, such as the Huanghe River, Liaohe River, and Luanhe River, flow into the BHS and transport large amounts of nutrients (Wang et al., 2019b). The BHS is a relatively closed environment with low self-purification capacity and is susceptible to human pressure (Wang et al., 2019b; Zhou et al., 2021). The BHS has a complex and changeable ocean circulation system, which exhibits a remarkable seasonal variation. The winter current field consists of cyclonic gyres in the southern BHS and off Qinhuangdao and anticyclonic gyres in the LDB and the central Bohai Sea. The summer current field is characterized by an anticyclonic gyre over the central shoal and two-layer overturning circulations in the coastal bays. The summer circulation is typically more complex due to the presence of stratification and the remarkable intraseasonal variability (Huang et al., 1999; Wu et al., 2023). In early summer, due to stronger southerly winds, a weak thermal gradient, and reduced intrusion of water from the North Yellow Sea (NYS), the BHS circulation is largely isolated within the basin, resulting in poor water exchange with the NYS. In late summer, the water from the NYS intrudes into the BHS, greatly altering the water supply in the BHS, especially in the southern regions (Wu et al., 2023). In the phytoplankton communities in the BHS, diatoms account for the highest proportion (65.3%–99.8%) of the annual average phytoplankton abundance, and the proportion in winter is up to 99.0% (Luan et al., 2018). The abundance of dinoflagellates in the BHS is much lower than that of diatoms during most of the year, but a higher value appears in summer or autumn, which can be several times that of diatoms (e.g., 4.65 times in the summer of 2000) (Luan et al., 2018).

In recent decades, the BHS has been experiencing environmental threats such as offshore oil and gas pollution, discharge of urban wastewater and sewage, and inputs of terrestrial pollutants and nutrients (Yu et al., 2021). The nutrient structure in the BHS has evolved from a low-nitrogen oligotrophic state (nitrogen limitation) before the 1990s to a low phosphorus eutrophication state (phosphorus and silicon limitations) (Wang et al., 2019b; Xin et al., 2019). The nitrogen-to-phosphorous molar ratio (hereinafter referred to as N/P ratio) exceeded the Redfield ratio of 16:1 since the 1990s and increased more rapidly after the year 2000 (Wang et al., 2019b). Many studies have reported a shift in the phytoplankton communities in the BHS from diatom dominance to a co-dominance of diatoms and dinoflagellates over the past few decades, concluding that this change is driven by long-term changes in nutrient structure (Sun et al., 2002; Xu et al., 2010). The abundance ratio of dinoflagellates to diatoms in the first 15 years of the 21st century was approximately 2.82 times that in the 20th century (Luan et al., 2018). The chlorophyll *a* concentration in the BHS showed an overall increasing trend in the past 20 years (1998–2018), and that in summer (June–August) increased the most, as high as 44.8% (Tian et al., 2019). Moreover, the phytoplankton communities in the BHS exhibited a trend of miniaturization, as evidenced by the shift towards nano- and pico-phytoplankton (Wang et al., 2018; Wei et al., 2021). Sun et al. (2019b) suggested that the shift in phytoplankton size structure was linked not only to the change in nutrient structure but also to climate change. Besides, changes have also been observed in the dominant species composition, diversity, and ecological characteristics of phytoplankton in the BHS since the 1990s. In the 20th century, large-sized centric diatoms (e.g., *Chaetoceros* spp. and *Coscinodiscus* spp.) were dominant, while after 2000, other centric diatoms (e.g., *Paralia sulcata*), pennate diatoms (e.g., *Thalassionema* spp. and *Navicula* spp.), and dinoflagellates (e.g., *Noctiluca scintillans* and *Tripos* spp.) emerged as dominant species (Luan et al., 2018). From the standpoint of nutrient limitation, the phosphorus-limited phytoplankton species declined while the nitrogen-limited species increased in the BHS (Xu et al., 2010). The Margalef's species richness and Shannon-Weiner diversity in the BHS declined sharply from the 1960s to the 2000s but recovered from the 2000s to the 2010s, while Pielou's evenness remained stable from the 1960s to the 2000s and dropped by 23% from the 2000s to the 2010s (Luan et al., 2018). The changes in phytoplankton biomass as well as in taxonomic composition in the BHS have resulted in a series of ecosystem problems, such as harmful algal blooms, oxygen depletion, and loss of zoobenthos (Song et al., 2016; Wang et al., 2018).

As described above, the phytoplankton community structure and diversity in the BHS underwent significant changes from the 1990s to the early 2010s in response to the drastic environmental changes. However, it remains unclear whether these historical trends in environmental conditions and phytoplankton community structure and diversity persisted, and further investigation is necessary. This study aims to analyze the temporal trends in the community structure and diversity of net-collected phytoplankton in the BHS and to investigate the relationship between these trends and environmental changes. The findings of this study will provide perspectives into the adaptive strategies of coastal ecosystems in response to environmental changes, and will also provide a scientific basis for the ecological protection of the BHS.

2 Materials and methods

2.1 *Study area and sampling*

The data for the present study are derived from 9 cruises in the BHS in August from 2011 to 2020. A total of 27 sites were set up covering the entire BHS, including LDB, BHB, LZB, and the CB, except for those in 2019, which only covered part of the BHS, primarily focusing on LDB and LZB. The sampling sites were not completely the same among years (Fig. 1, Table S1).

Observations and samplings of the physical and chemical factors were synchronously carried out with the biological sampling on the same vessel each year. Temperature, salinity, depth, and pH were measured *in situ* using a Conductivity-Temperature-Depth (CTD) system (SeaBird, USA), while water samples were obtained at different depths utilizing a multi-bottled water sampler. The depth layers for the observations of physical and chemical factors were selected by the criteria in Table S2. Dissolved oxygen (DO) was determined onboard using iodometric titration according to the National Standard of China (GB/T 17378.4–2007). A seawater subsample (500 mL each) from each depth layer was filtered through a 0.7 μm GF/F filter (Whatman, UK) under a vacuum pressure of less than 50 kPa for the measurement of chlorophyll *a* (Chl *a*). The filtered seawater was then collected into 100 mL polyethylene terephthalate (PET) bottles and frozen at –20℃ for quantitative analysis of nutrients.

The phytoplankton sample at each site was collected by towing a plankton net (76 μm mesh size, 37 cm mouth diameter) vertically from 2 m above the seafloor to the surface at a speed of 0.5 m/s. The volume of filtered water was determined by mul-

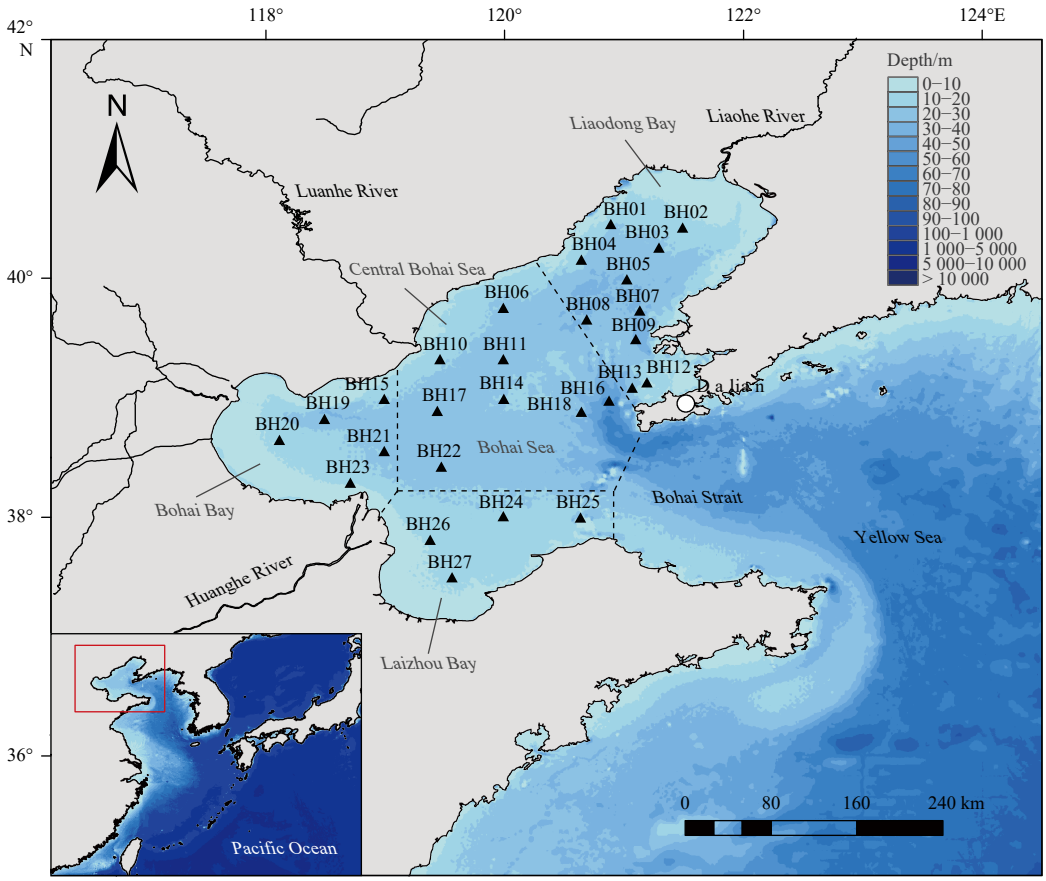

Fig. 1. The geographic location of the study area and sampling sites. The sites belonging to different regions of the BHS, namely Liaodong Bay, Bohai Bay, Laizhou Bay, and the central Bohai Sea, are separated by dashed lines.

tiplying the rope length by the mouth area. The phytoplankton samples were placed in 1 L polyethylene bottles and preserved by adding formaldehyde (final concentration 5%) before being transported to the laboratory for subsequent analysis. The phytoplankton species that were expected to be captured belonged to the micro-phytoplankton category. Zooplankton samples at each site were collected by vertically trawling plankton Net Ⅰ (505 μm mesh size, 50 cm mouth diameter) and Net Ⅱ (160 μm mesh size, 32 cm mouth diameter), respectively, which were then kept in 500 mL polyethylene bottles and fixed with a formaldehyde solution (final concentration 5%). The phytoplankton and zooplankton samplings were referred to the National Standard of China (GB/T 12763.6–2007).

2.2 *Laboratory analysis*

In the laboratory, Chl *a* extraction was carried out in 5 mL 90% acetone (4℃ for 24 h in the dark). After removing the filters, Chl *a* concentration was measured on a fluorometer (Turner Designs, USA) following the method of Welschmeyer (1994). The water samples for nitrate (NO_3^--N), nitrite (NO_2^--N), ammonium (NH_4^+-N), phosphate (PO_4^{3-}-P), and silicate (SiO_3^{2-}-Si) were measured by continuous flow analyzer (AA3, Seal Analytical, Germany). N/P ratio was calculated by dividing the molar concentration of dissolved inorganic nitrogen (DIN: NO_3^--N, NO_2^--N, and NH_4^+-N) by the molar concentration of dissolved inorganic phosphorus (DIP: PO_4^{3-}-P). Nitrogen-to-silicon molar ratio (hereinafter referred to as N/Si ratio) was calculated by dividing the molar concentration of DIN by the molar concentration of dissolved silica (DSi: SiO_3^{2-}-Si).

For enumeration and identification of phytoplankton cells, an aliquot with a certain volume (ensuring that no less than 200 cells were observed) from each phytoplankton sample was examined in an Utermöhl chamber. All samples were examined using an Olympus CKX53 inverted microscope (Olympus, Tokyo, Japan). Each species was identified to the lowest possible taxonomic level. The validity of taxonomic names and synonyms was checked with the website AlgaeBase (http://www.algaebase.org). Zooplankton samples were manually identified to the species level based on expert knowledge and were counted under a dissecting microscope (Leica, Germany). The abundance of phytoplankton/zooplankton for each sample was obtained by dividing the number of phytoplankton/zooplankton individuals by the volume of filtered water.

2.3 *Data analysis*

The vertical temperature gradient (hereinafter referred to as gradient) was calculated by Eq. (1) to characterize the thermocline intensity (Zhou et al., 2009):

$$\text{Gradient} = (T_\text{b} - T_\text{s})/\text{Depth}, \tag{1}$$

where T_b is bottom temperature; T_s is surface temperature; and Depth is water column depth.

The eutrophication index (EI) was calculated by Eq. (2):

$$\text{EI} = (C_\text{COD} \times C_\text{N} \times C_\text{P} \times 10^6/4\,500), \tag{2}$$

where C_COD is the concentration (mg/L) of chemical oxygen de-

mand (COD), C_N is DIN concentration (mg/L), and C_P is DIP concentration (mg/L).

The mean values of the environmental variables across layers were calculated for each site and were used in subsequent analyses. Local regression (LOESS), known for its unique ability to reveal complex patterns and non-linear trends, was employed to assess the trends in environmental variables and the relationships between phytoplankton taxa and key environmental factors. The regression analysis was visualized with R (R Core Team, 2018).

To describe the phytoplankton community structure, the diversity indices including Margalef's richness (D) (Margalef, 1968), Shannon-Wiener diversity (H') (Shannon and Weaver, 1949), and Pielou's evenness (J) (Pielou, 1966) were calculated using the Vegan Package according to Eqs (3)–(5). The dominance (Y) index of species (Sun et al., 2004b) was calculated according to Eq. (6):

$$D = (S-1)/\log_2 N, \tag{3}$$

$$H' = -\sum_{i=1}^{S}(n_i/N)\log_2(n_i/N), \tag{4}$$

$$J = \frac{H'}{\log_2 S}, \tag{5}$$

$$Y = \frac{n_i}{N} f_i, \tag{6}$$

where S is total number of species, N is total number of individuals, n_i is abundance of the ith species, and f_i is occurrence of the ith species. Species with $Y \geqslant 0.02$ were considered as dominant species in the studied area (Sun et al., 2004b).

The Dia/Dino index, which reflects the dominance pattern in the phytoplankton composition, was calculated by Eq. (7) (Mokrane et al., 2019):

$$\text{Dia/Dino index} = Ab_{\text{Dia}}/(Ab_{\text{Dia}} + Ab_{\text{Dino}}) \tag{7}$$

where Ab_{Dia} is diatom abundance and Ab_{Dino} is dinoflagellate abundance. The Dia/Dino index values range from 0 to 1.

The multiple comparisons of phytoplankton abundance and diversity indices among years were conducted using R. Firstly, the Shapiro-Wilk and Levene's tests were performed to assess the normality and homogeneity of variance using the Stats and Car packages, respectively. Subsequently, the Kruskal-Wallis test was employed to determine significant differences among years using the Stats Package. A post-hoc Nemenyi test was then performed using the PMCMRplus Package with a Benjamini-Hochberg P-value adjustment to make pairwise comparisons. The statistical significance level for hypothesis testing of differences was set at $p < 0.05$.

Redundancy analysis (RDA) was carried out using the Vegan Package based on square root-transformed phytoplankton composition data and $\log_{10}(X+1)$-transformed environmental data (pH data were not transformed) since the Shapiro-Wilk test showed nonnormal distributions of phytoplankton abundance and environmental variables. First, variance inflation factors (VIFs) of variables were calculated, and variables with VIF > 10 were excluded from RDA to avoid the collinearity problem. Then, the significant explanatory variables ($p < 0.05$) were determined by forward selection (FS) using the Packfor Package (Blanchet et al., 2008). Spearman correlation analysis was performed using the Hmisc Package to assess the relationship between phytoplankton taxa and diversity indices/environmental variables. The statistical significance level for correlation analysis was set at $p < 0.05$.

3 Results

3.1 *Variations in environmental factors*

The temperature (range 22.19–25.03℃), salinity (range 29.07–31.51), and PO_4^{3-}-P concentration (range 0.08–0.35 μmol/L) in the BHS during August 2011–2020 generally showed upward trends, while the pH (range 8.05–8.28), gradient (0.07–0.35℃/m), DIN concentration (range 4.01–12.81 μmol/L), N/P ratio (range 14.07–138.35), and N/Si ratio (range 0.38–1.16, no data for 2011–2013) exhibited downward trends (Fig. 2). Both temperature and salinity reached their highest levels in August 2017 (Fig. 2a and b). gradient reached its highest in August 2013 (Fig. 2e). The Chl *a* concentration (range 1.03–4.57 μg/L, no data for 2011) decreased first and then increased in 2020 (Fig. 2l). No obvious trends were observed in DO concentration (range 6.24–7.79 mg/L), SiO_3^{2-}-Si concentration (range 5.94–17.07 μmol/L, no data for 2011–2013), EI (range 0.07–0.26), Net Ⅰ zooplankton abundance (range 0.15–0.46 ind./L, no data for 2016) , and Net Ⅱ zooplankton abundance (range 7.27–27.88 ind./L, no data for 2016) over the monitoring period (Fig. 2).

We noticed that the N/P ratio was highly variable during the monitoring period (Fig. 3). Before 2016, the N/P ratio in the BHS ranged from 14.1 to 686.6, with a median of 55.9, and more than 98% of the observed values were higher than the Redfield ratio of 16:1 (values lower than 16:1 were observed only at Site BH14 in the CB). The N/P ratio in the BHS in late summer has decreased markedly since 2016, ranging from 3.3 to 83.2 with a median value of 17.2, which was closer to 16:1 compared to the period before 2016.

3.2 *Variations in phytoplankton communities*

3.2.1 *Community composition and abundance*

A total of 152 phytoplankton taxa (including unidentified species) were identified from all the phytoplankton samples, belonging to three phyla, i.e., Bacillariophyta (109 species, 48 genera), Dinoflagellata (41 species, 10 genera) and Ochrophyta (2 species, 2 genera) (Table S3). At the genus level, *Chaetoceros* had the highest richness (26 species), followed by *Protoperidinium* (15 species), *Coscinodiscus* (12 species), and *Tripos* (10 species).

The total phytoplankton abundance peaked in 2019 (32 342 cells/L) mainly due to the extremely high abundance in the LDB, while the total abundance was the lowest in 2020 (273 cells/L) due to the low values throughout the BHS (Fig. 4d, g and 5, Table S4). At the phylum level, the abundance of Bacillariophyta accounted for the highest proportion of the total abundance during the study period, ranging from 53.2% to 99.5%. The abundance of Bacillariophyta exhibited a similar trend with the total abundance, peaking in 2019 (32 156 cells/L), primarily driven by a notably high abundance in the LDB, and reaching a minimum in 2020 (216 cells/L) (Fig. 4a). Dinoflagellata accounted for less than 10% of the total abundance except for the late summers of 2016 (46.8%) and 2017 (27.5%) (Fig. 4b). The abundance of Dinoflagellata peaked in 2016 (674 cells/L), followed by 2017 (474 cells/L), and was the lowest in 2018 (41 cells/L) and 2020 (57 cells/L). The

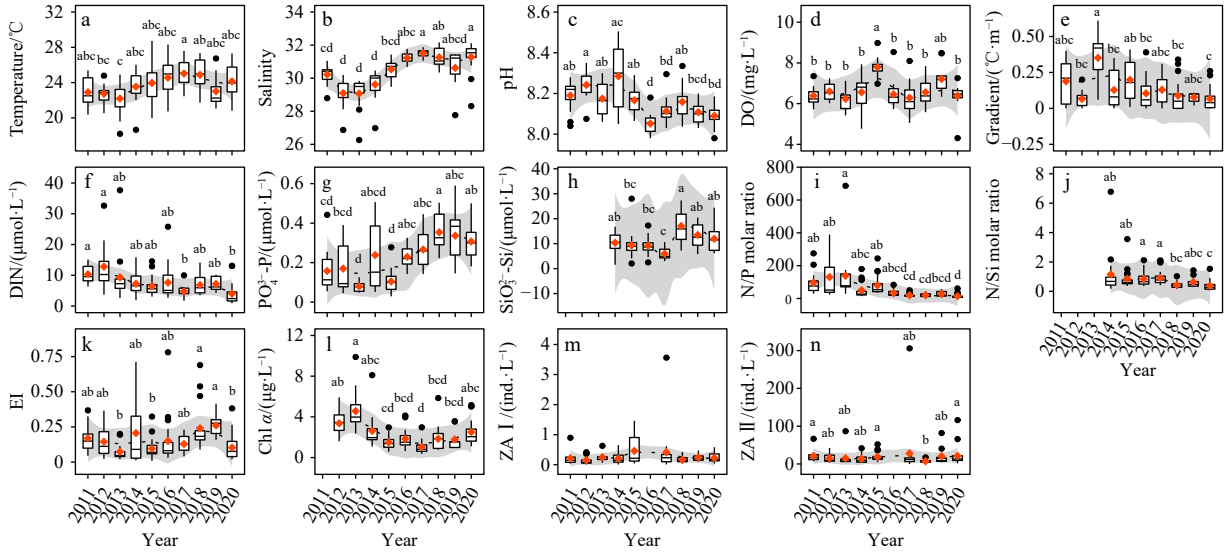

Fig. 2. Temporal variations in the main environmental factors in the BHS during August 2011–2020. Data are presented in box and whisker plots. The black points represent the outliers, and the orange points are the mean values. The solid lines are the LOESS regression lines, reflecting their dynamic trends during the study period, and gray shadows denote the 95% confidence intervals. The letters above bars indicate differences between years and the absence of the same letters indicates a significant difference (Nemenyi test: $p < 0.05$). There is no significant difference in the Net Ⅰ zooplankton abundance across years. The abbreviations of the environmental variable names are as follows: DO: dissolved oxygen; DIN: dissolved inorganic nitrogen; EI: eutrophication index; Chl *a*: chlorophyll *a*; ZA Ⅰ: Net Ⅰ zooplankton abundance; ZA Ⅱ: Net Ⅱ zooplankton abundance.

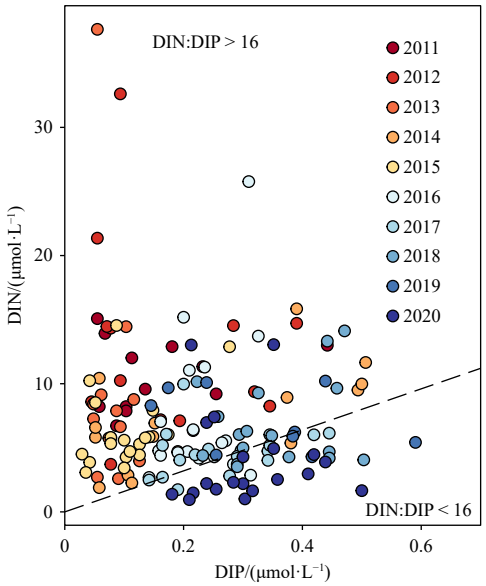

Fig. 3. Changes in the relationship between dissolved inorganic nitrogen (DIN) and dissolved inorganic phosphorus (DIP) in the BHS during August 2011–2020. The dashed line represents the Redfield ratio (N/P ratio = 16:1).

highest abundances of Dinoflagellata were recorded in the BHB in 2016 and in the CB in 2017, respectively (Fig. 4g). Ochrophyta accounted for only 0–0.07% of the total phytoplankton abundance across years, and its abundance ranged from 0.2 cells/L (2020) to 4 cells/L (2012) (Fig. 4c). Due to the extremely low relative abundance of Ochrophyta in the BHS, the subsequent analyses focused on the dominant groups Bacillariophyta and Dinoflagellata rather than Ochrophyta. The average Dia/Dino index peaked in 2019 (0.94) and reached its lowest point in 2013 (0.62) (Fig. 4e). The lower average Dia/Dino index in 2013 was due to the lower Dia/Dino indices in the LZB and the CB, however, no significant differences were found among years in the entire BHS, as well as in each specific region of the BHS (Fig. 4g). The average Dia/Dino index in the CB (0.69) was lower than that in the LDB (0.83), BHB (0.80), and LZB (0.89) (Table S4). At the genus level, *Skeletonema* (absolute abundance: 2–25 124 cells/L, relative abundance: 0.07%–77.68%), *Chaetoceros* (absolute abundance: 59–5 038 cells/L, relative abundance: 8.73%–79.38%), *Pseudo-nitzschia* (absolute abundance: 11–1 036 cells/L, relative abundance: 0.59%–21.07%), *Eucampia* (absolute abundance: 0.2–2 309 cells/L, relative abundance: 0.004 5%–29.76%), and *Tripos* (absolute abundance: 38–645 cells/L, relative abundance: 0.41%–44.75%) had higher abundances. It was noteworthy that the genera *Skeletonema* and *Eucampia* each consisted of only one species, i.e., *Skeletonema costatum* and *Eucampia zoodiacus*, respectively.

3.2.2 *Diversity*

The diversity indices (total species number, Margalef's richness, Shannon diversity, and Pielou's evenness) fluctuated during the study period, and the median values of all four indices were at their lowest in the late summer of 2015 (Fig. 6a, Table S5). Kruskal-Wallis nonparametric test showed that total species number, richness, and evenness were significantly different among years (Fig. 6a). Total species number in 2012 was significantly greater than that in 2013, 2015, and 2020. Margalef's richness in 2012 was significantly greater than that in 2015. Evenness in 2020 was significantly greater than that in 2015. No significant difference was found in Shannon diversity among years. Spearman correlation analysis indicated that the total phytoplankton abundance, the absolute/relative abundances of Bacillariophyta, and the Dia/Dino index were positively correlated with total species number but were negatively correlated with evenness (Fig. 6b). The relative abundance of Dinoflagellata, in contrast, had a negative correlation with total species number and a posit-

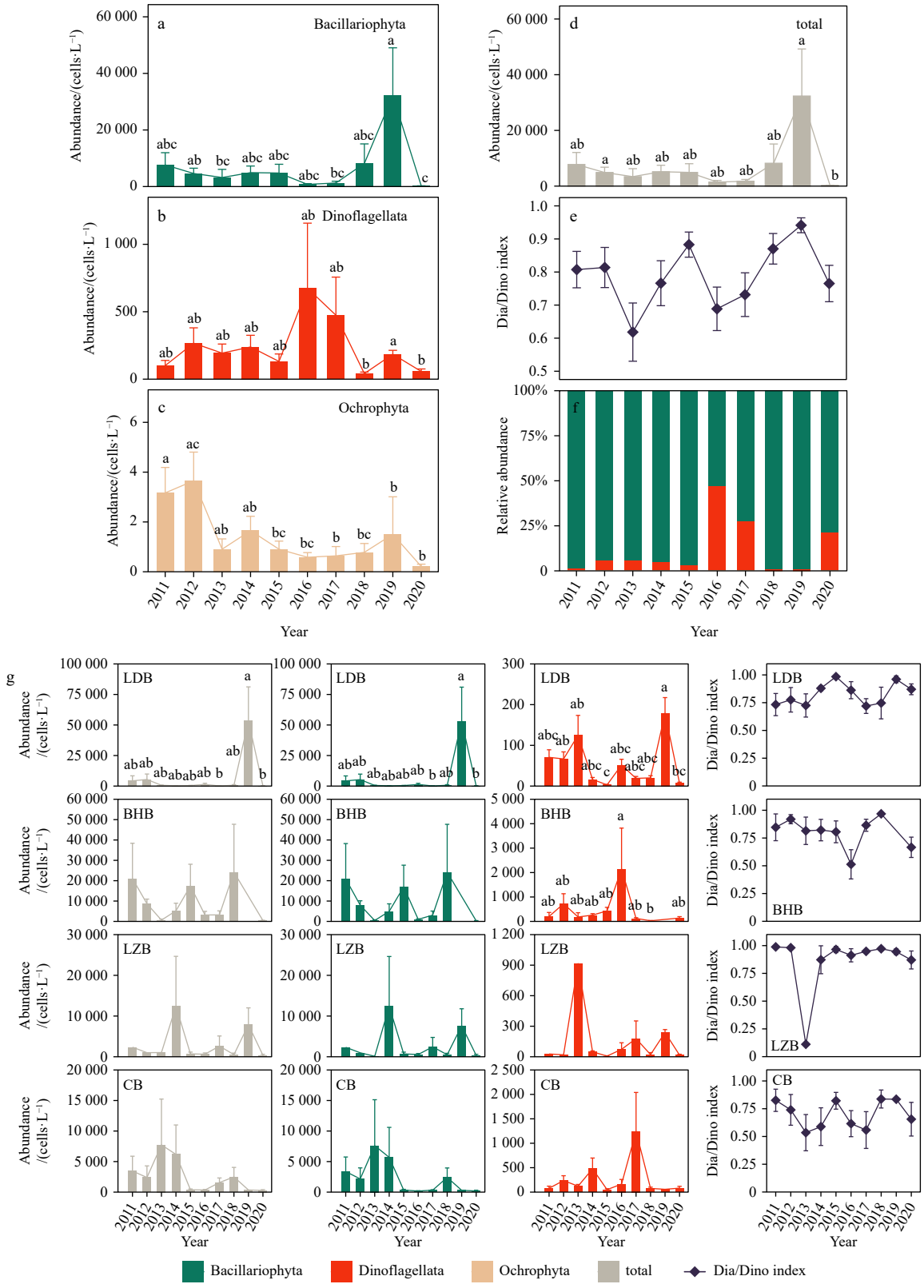

Fig. 4. Variations in phytoplankton abundance in the BHS during August 2011–2020. Panels a-f show the variations in the entire BHS, and panel g shows the variations in different regions of the BHS (LDB: Liaodong Bay; BHB: Bohai Bay; LZB: Laizhou Bay; CB: central Bohai Sea). The stacked barplots depict the relative abundances of phytoplankton phyla. In the barplots of the absolute abundances, bars and error bars represent means and standard errors, respectively. The letters above bars indicate differences between years and the absence of the same letters indicates a significant difference (Nemenyi test: $p < 0.05$). A lack of letter marks indicates no significant difference among years (Kruskal-Wallis test: $p > 0.05$). The Dia/Dino index is an exception, with a significant difference among years tested by the Kruskal-Wallis test but no significant difference tested by the Nemenyi test.

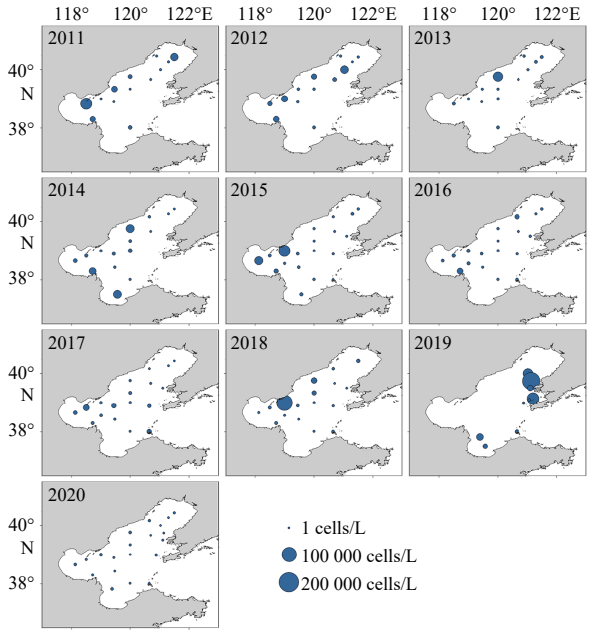

Fig. 5. Distributions of phytoplankton abundance in the BHS during August 2011–2020.

ive correlation with evenness (Fig. 6b).

3.2.3 *Dominant species*

A total of 21 phytoplankton species dominated the phytoplankton communities in the late summers of 2011–2020 (Fig. 7, Table S6). Among these, 11 species emerged as dominant species for more than 2 years, i.e., *Skeletonema costatum*, *Chaetoceros pseudocurvisetus*, *Chaetoceros lorenzianus*, *Chaetoceros curvisetus*, *Tripos muelleri*, *Paralia sulcata*, *Thalassionema frauenfeldii*, *Pseudo-nitzschia pungens*, *Eucampia zoodiacus*, *Ditylum brightwellii*, and *Chaetoceros compressus*, exhibiting different patterns in abundance and dominance over the 10 years (Fig. 7, Table S6). For example, *Skeletonema costatum* dominated the phytoplankton communities for 6 years, and its dominance was especially great in 2017–2019 (Fig. 7). *Skeletonema costatum* was recorded at a higher proportion of sites in the late summers of 2017–2019 and with higher abundances at specific nearshore sites in the late summers of 2018 and 2019 (Fig. S1). *Paralia sulcata* was dominant with higher abundances in the late summers of 2012, 2013, and 2015, and was no longer prevailing since 2016 (Figs 7, S2).

3.3 *Relationship between phytoplankton communities and environmental factors*

3.3.1 *Relationship between phytoplankton community composition/diversity and environmental factors*

According to the VIF values of the explanatory variables, the N/P ratio was excluded from the RDA models. FS determined that the variations in the absolute abundance of species were significantly correlated with DO, PO_4^{3-}-P, and DIN (Figs 8a and b), while the variations in the relative abundance of species were also significantly correlated with gradient, salinity, depth, DO, PO_4^{3-}-P, DIN, and pH (Figs 8c and d). The variations in absolute abundance of different phyla were significantly correlated with DO, DIN, Chl *a*, and PO_4^{3-}-P (Figs 8e and f), while the variations in relative abundance of different phyla were significantly correlated with gradient and DO (Figs 8g and h). The variation in diversity indices (total species number, Margalef's richness, Shannon diversity, Pielou's evenness) exhibited a significant positive correlation with temperature and PO_4^{3-}-P and a negative correlation with gradient (Fig. 8i).

3.3.2 *Relationship between phytoplankton groups/dominant species and environmental factors*

The Dia/Dino index and the absolute/relative abundances of Bacillariophyta exhibited a significant negative correlation with gradient and depth and a significant positive correlation with DO concentration and temperature (Figs 8f, i, S3). The absolute abundance of Dinoflagellata showed a significant positive correlation with the N/Si ratio and pH. The relative abundance of Dinoflagellata exhibited a positive correlation with gradient and depth and a significant negative correlation with DO and temperature (Figs 8f, h and i, and S3). Notably, the relative abundances of Bacillariophyta and Dinoflagellata were inversely related to depth, temperature, gradient, and DO concentration. In addition, both the Dia/Dino index and the relative abundance of Bacillariophyta showed a positive correlation with Net Ⅰ zooplankton abundance, while the absolute/relative abundances of Dinoflagellata exhibited a negative correlation with it (Fig. 8i). The absolute/relative abundances of Ochrophyta were positively correlated with N/P ratio and DIN and were negatively correlated with salinity and PO_4^{3-}-P concentration (Figs 8i, S3). Like Bacillariophyta, the absolute/relative abundances of the abundant genera within Bacillariophyta, including *Skeletonema*, *Pseudo-nitzschia*, and *Eucampia*, exhibited a significant negative correlation with gradient (Figs 8i, S4). The genus *Skeletonema* also exhibited a significant positive correlation with temperature and PO_4^{3-}-P concentration (Figs 8i, S4). The relative abundance of *Tripos* exhibited a significant positive correlation with depth and salinity and a negative correlation with DO and Chl *a* concentrations (Figs 8i, S4).

The absolute/relative abundances of *Skeletonema costatum* had a positive correlation with temperature, PO_4^{3-}-P and EI and a negative correlation with gradient (Fig. 8i). The absolute/relative abundances of *Paralia sulcata* were significantly and positively correlated with depth, gradient, and N/P ratio and were negatively correlated with temperature and PO_4^{3-}-P concentration (Fig. 8i). The absolute/relative abundances of *Tripos longipes* were strongly and positively correlated with salinity, PO_4^{3-}-P and depth, and were negatively correlated with N/P ratio, Chl *a* concentration and pH (Fig. 8b, d, and i). Remarkably, this species started to occur in the studied area since 2016 and was dominant in the late summer of 2017 (Fig. S5).

4 Discussion

4.1 *The relationship between phytoplankton groups and environment*

The relationship between phytoplankton communities and environmental factors in the BHS was studied using nonlinear (Spearman) and linear (RDA) correlations. Correlations may not reveal cause-and-effect relationships directly, but parsing correlation results based on relevant knowledge can help speculate and understand potential relationships.

The results indicated a close association between the phytoplankton communities and nutrient structure in late summer. Specifically, the higher phytoplankton abundance was associated with higher DIN concentration, N/P ratio, and N/Si ratio, while the greater diversity was associated with a higher PO_4^{3-}-P

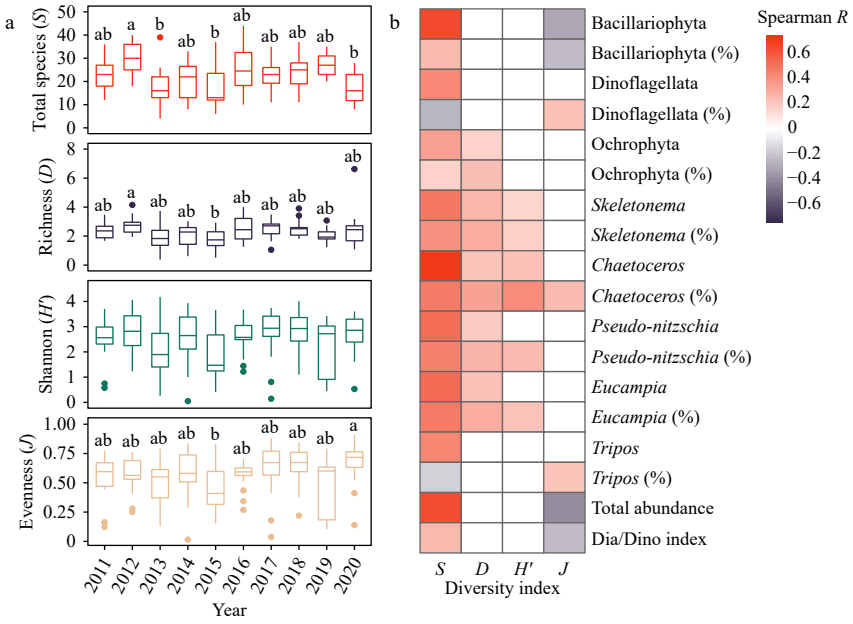

Fig. 6. Phytoplankton diversity in the BHS during August 2011–2020. a. Variations in diversity indices (total species number, Margalef's richness, Shannon diversity, Pielou's evenness). Boxes depict medians and upper/lower quartiles; whiskers depict ranges and points are outliers. The letters above the boxes indicate differences between years and absence of the same letters indicates a significant difference (Nemenyi test: $p < 0.05$). There is no significant difference in Shannon diversity across years. b. Spearman correlation between phytoplankton diversity indices and the abundances of taxonomic groups. Taxa indicated with "%" in parentheses represent relative abundances, while those without "%" denote absolute abundances. Red and gray cells represent significant positive and negative correlations respectively ($p < 0.5$), and blank cells represent nonsignificant correlations ($p \geqslant 0.5$).

concentration. This reflects the positive effects of nutrient levels on phytoplankton growth and diversification. The relative abundance of Bacillariophyta was found to be positively correlated with total species number and negatively correlated with evenness, while the relative abundance of Dinoflagellata showed the opposite pattern, suggesting the different effects of diatoms and dinoflagellates on phytoplankton diversity in the BHS during the study period. Diatom dominance tended to increase the total species number and resulted in a non-equilibrium abundance distribution among species, characterized by a few diatom species exhibiting extremely high abundances, while the majority of species showed relatively low abundances. In contrast, dinoflagellate dominance tended to promote a more balanced distribution of abundances among species, resulting in less disparity in abundance across the various species. This was mainly due to the different survival strategies of diatoms and dinoflagellates, which are reflected in different growth rates, nutrient absorption rates, and migration capabilities (Smayda, 2002; Wasmund et al., 2017).

The results also showed that the correlations between the Dia/Dino index and nutrient concentrations (DIN, PO_4^{3-}-P, SiO_3^{2-}-Si) or element ratios (N/P ratio, N/Si ratio) were weak. Instead, the Dia/Dino index was negatively correlated with water column depth and gradient (representing thermocline intensity), while it exhibited positive correlations with temperature, DO concentration, and Net Ⅰ zooplankton abundance. Moreover, the lowest value of the Dia/Dino index and the highest gradient occurred simultaneously in the late summer of 2013. The correlation of the Dia/Dino index with depth and gradient aligns with previous knowledge about the ecological niches of diatoms and dinoflagellates; specifically, diatoms are better adapted to well-mixed water columns, whereas dinoflagellates are adapted to stratified waters with low turbulence (Smayda, 2002; Xiao et al., 2018). In August, the thermocline thickness and gradient in the BHS are reducing but still relatively strong, and the gradient correlates with water column depth (Zhou et al., 2009). Therefore, the Dia/Dino index exhibited a negative correlation with both depth and gradient. The lower Dia/Dino ratio in the CB than in the three bays was also due to the greater water column depth and stronger stratification in the CB. However, contrary to the previous view that diatoms prefer low-temperature water while dinoflagellates are insensitive to temperature (Alexander, 2016), the Dia/Dino index was positively correlated with temperature in the BHS. This was due to the strong correlation between the mean water column temperature and the gradient/depth (Fig. S6), indicating that stratification played a more significant role than temperature in determining the relative dominance of diatoms and dinoflagellates.

The correlation between the Dia/Dino index and DO concentration reflected the different effects of diatoms and dinoflagellates on the environment rather than responses to the environmental changes. DO concentration is largely determined by vertical mixing (Obenour et al., 2012), temperature (Carstensen et al., 2014), and biological factors (Rabalais et al., 2014). Phytoplankton can contribute to DO, but DO has relatively weak effects on phytoplankton. Both diatoms and dinoflagellates produce oxygen through photosynthesis, but diatoms have a higher photosynthetic rate per unit carbon compared to dinoflagellates (Chan, 1980). The heterotrophic and mixotrophic groups of dinoflagellates do not produce oxygen during their heterotrophic life stage, also resulting in a lower oxygen production rate of dinoflagellates than diatoms. Certain taxa that occurred at high abundances or formed blooms can lead to increased oxygen production. For example, *Skeletonema costatum* bloomed (abundance 120 851 cells/L) and *Chaetoceros pseudocurvisetus* occurred with a high abundance (25 510 cells/L) at Site BH07 in August 2019, which corresponded with an elevated DO concentration (8.48 mg/L).

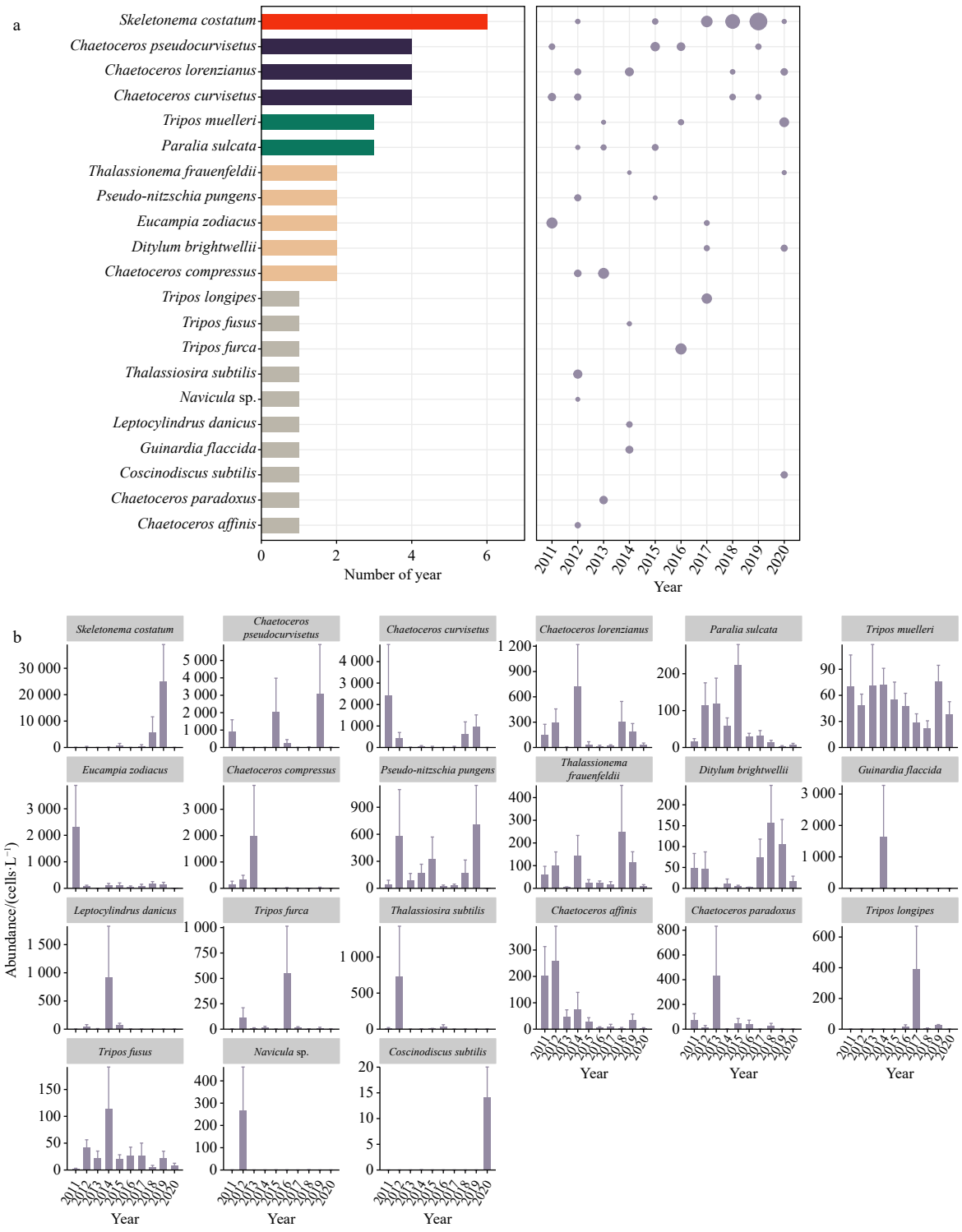

Fig. 7. Variations in dominant phytoplankton species in the BHS during August 2011–2020. a. Bars indicate the number of years in which the species appear as dominant species ($Y \geqslant 0.02$), and points indicate Y values of the dominant species (only $Y \geqslant 0.02$ are shown). b. Bars represent the mean abundances of the dominant species and error bars represent standard errors.

The significant correlation of pH with the community composition, as well as the abundances of certain taxa—such as Dinoflagellata, *Tripos longipes*, and *Paralia sulcata*—was likely to reflect the different responses of different taxa to environmental changes, and some taxa might be more sensitive to pH changes than others.

The results also suggested that the Net Ⅰ zooplankton abundance exhibited a positive correlation with the Dia/Dino index and a negative correlation with the absolute/relative abundances of dinoflagellates, especially *Tripos*, which was the most abundant genus within Dinoflagellata. The zooplankton abundance in this study was obtained based on samples collected by both Net Ⅰ and Net Ⅱ for more comprehensive information, because Net Ⅰ is inefficient for collecting smaller individuals (e.g.,

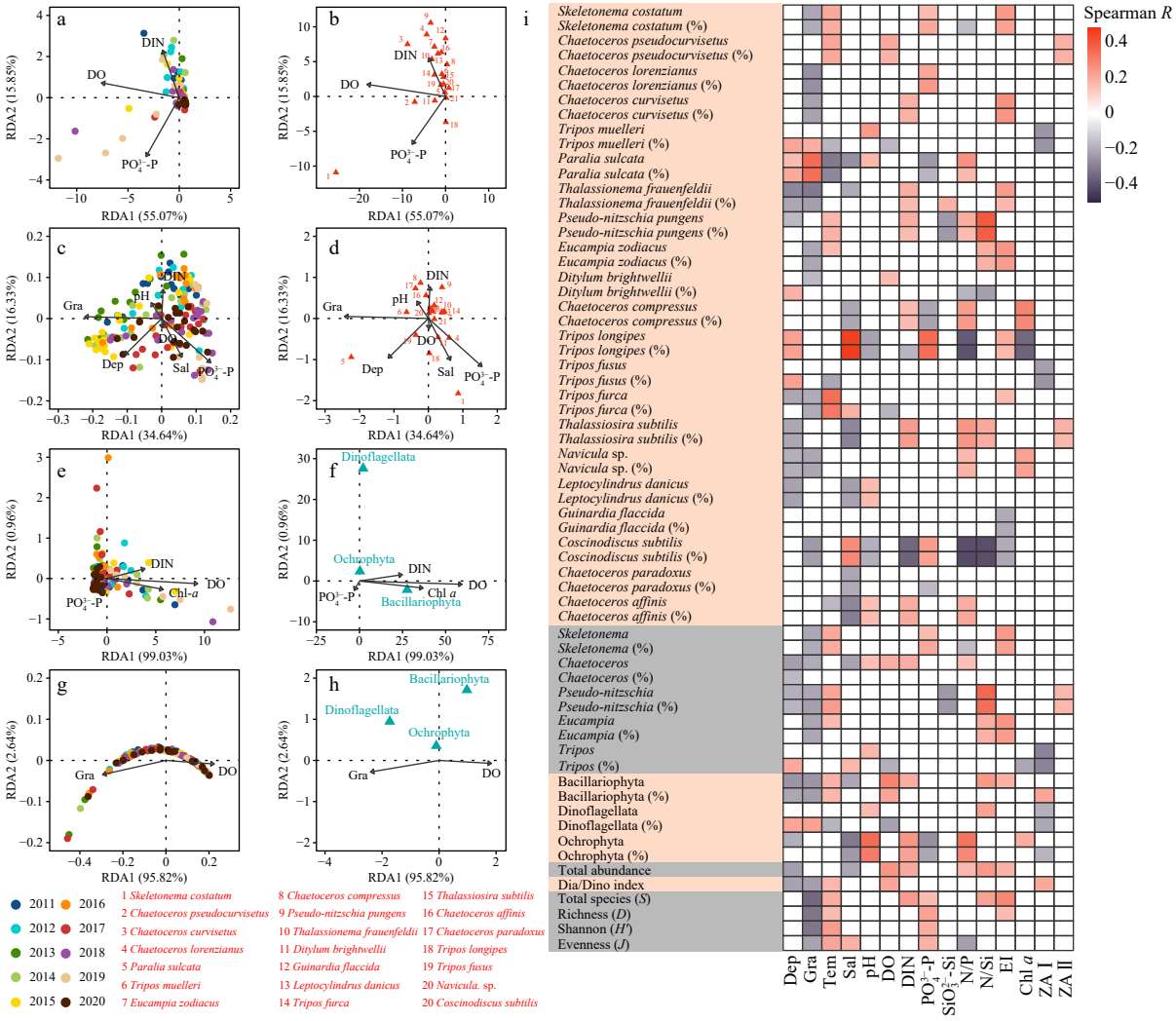

Fig. 8. Relationship between the phytoplankton communities and environmental factors in the BHS during August 2011–2020. RDA biplots show the relationship between phytoplankton samples (a, c, e, g)/taxa (b, d, f, h) and significant explanatory variables. a and b are based on the absolute abundance of species. c and d are based on the relative abundance of species. e and f are based on the absolute abundance of phyla. g and h are based on the relative abundance of phyla. i Heatmap showing the Spearman correlations between the dominant phytoplankton species and environmental factors. Taxa indicated with "%" in parentheses represent relative abundances, while those without "%" denote absolute abundances. Red and gray cells represent significant positive and negative correlations ($p < 0.5$), respectively, and blank cells represent nonsignificant correlations ($p \geqslant 0.5$). The abbreviations of the environmental variable are as follows: Dep: depth; Gra: gradient; N/P: N/P molar ratio; N/Si: N/Si molar ratio; Sal: salinity; Tem: temperature; ZA Ⅰ: Net Ⅰ zooplankton abundance; ZA Ⅱ: Net Ⅱ zooplankton abundance. See the caption of Fig. 2 for other abbreviations.

hydromedusa, copepods, and zooplankton larvae) but is more advantageous for collecting larger individuals (e.g., mysis, decapods) compared to Net Ⅱ (Ge et al., 2019). *Tripos* are considered as constitutive mixotrophs, meaning that they have the capacity to acquire energy through photosynthesis but can also consume other organisms when the macro-nutrients required for photosynthesis are depleted (Anderson et al., 2022). The observed relationship between Net I zooplankton abundance and the Dia/Dino index, or dinoflagellate abundance, might be due to the importance of diatom dominance in supporting the growth of large-sized zooplankton (>505 μm). There might also be antagonistic relationships between dinoflagellates and large-sized zooplankton, such as competition for prey. Besides, the RDA results indicated that the community variation at the phylum level was primarily associated with factors (e.g., DIN, gradient) other than zooplankton abundance. The findings above together indicate that the bottom-up effect played a key role in structuring the phytoplankton communities during the study period. However, the interactions between phytoplankton and zooplankton are extraordinarily complex (Straile, 1997), and our data can only provide a glimpse into the net effects of interactions between diverse phytoplankton and zooplankton groups.

4.2 *The phytoplankton species strongly associated with environmental changes in the BHS*

By analyzing the trends of the dominant phytoplankton species and their correlations with the environmental factors in the BHS, we found that certain species responded sensitively to specific environmental changes and warrant further attention.

Skeletonema costatum was reported with a decreased dominance from the 20th century to the beginning of the 21st century in the BHS (Luan et al., 2018), whereas our results showed that the

dominance of *Skeletonema costatum* rose in the late summers of 2017–2019. Particularly, the cell density of *Skeletonema costatum* in the LDB (at Sites BH05, BH07, and BH12) in 2019 was above the cell density threshold for bloom (1×10^4 cells/L). The absolute/relative abundances of *Skeletonema costatum* were found to be positively correlated with water temperature, PO_4^{3-}-P, and EI, and its relative abundance was negatively correlated with the N/P ratio. The optimum N/P ratio of *Skeletonema costatum* was 16:1 (Liu et al., 2002), and the N/P ratio in the BHS declined to near this ratio from the year *Skeletonema costatum* became prevalent. Therefore, the decrease in the N/P ratio might be the decisive factor for the increase in the dominance of *Skeletonema costatum*.

Paralia sulcata is a heavily silicified and small-sized diatom species, which is frequently observed in both the planktonic and benthic communities in coastal waters (Gebühr et al., 2009; Liu and Glibert, 2018). From the beginning of the 21st century to 2015, there was a noticeable increase in both the abundance and dominance of *Paralia sulcata* in the BHS, with a particularly significant contribution in the CB (Liu and Glibert, 2018; Luan et al., 2018). Some studies have linked its predominance in the BHS to the water-sediment regulation of the primary river, the Huanghe River (Luan et al., 2018), as well as the influence of the Yellow Sea Warm Current (YSWC) (Liu et al., 2015b; Wang et al., 2019a). Our study found an obvious decline in the abundance and dominance of *Paralia sulcata* after 2015. Its absolute/relative abundances were found to be positively correlated with depth, gradient, and N/P ratio, while negatively correlated with water temperature and PO_4^{3-}-P concentration. This is roughly consistent with the previous reports that *Paralia sulcata* occurs under conditions of low temperature and N/P ratio, and high N/Si ratio (Liu and Glibert, 2018). Compared with other diatoms, *Paralia sulcata* has the advantage that it does not suffer from severe phosphorus stress in phosphorus-deficient waters (Wang et al., 2014; Yu et al., 2015), such as high N/P ratio or stratified waters that is unfavorable for the growth of most diatoms. This may explain why the abundance and dominance of *Paralia sulcata* decreased significantly with the decrease of the N/P ratio in the BHS in late summer, especially since 2016. Moreover, the decline in temperature was also detrimental to the maintenance of its dominance.

Tripos longipes occurred continuously in the BHS during the late summers of 2016–2020 and appeared as a dominant species in the late summer of 2017. This species exhibited significant correlations with multiple environmental factors, especially with salinity, PO_4^{3-}-P, pH, DIN, and Chl *a*. *Tripos longipes*, which is also recorded as *Tripos horridus* in some literature, is reported to be widely distributed in coastal and oceanic, cold to warm temperate waters with its abundance related to greater salinity and transparency (Burns and Mitchell, 1982; Ke et al., 2014; Liu et al., 2015a; Zakaria et al., 2016; Luan et al., 2020). *Tripos longipes* was rarely reported to occur in the BHS but has been found in the Yellow Sea, which is adjacent to the BHS (Li et al., 2015; Liu et al., 2015a; Luan et al., 2020), and in the Bohai Strait, which is the only pathway between the BHS and the Yellow Sea (Sun et al., 2004a). Recent reports suggested that the YSWC, characterized by higher temperature, salinity, and phosphate concentration, has been increasing in intensity in recent years, particularly in 2017, and could have an increasing impact on the BHS (Cao and Zhu, 2021; Yu et al., 2020). In line with this, our data also showed that the temperature, salinity, and phosphate concentration in the late summer of 2017 were higher. In addition, the reduced runoff into the BHS has led to an increase in salinity in the BHS (Shi et al., 2020). Thus, the increase in *Tripos longipes* dominance in the BHS in recent years was mostly related to the increase in salinity and PO_4^{3-}-P concentration, which resulted from the changes in the intrusion intensity of the Yellow Sea waters and the runoff into the BHS. However, this potential correlation requires confirmation through physiological studies on this species.

4.3 *Environmental changes and trends in the BHS in late summer*

Under the influence of dense human activities combined with changes in the natural environment, the environmental changes in the BHS have been attracting considerable attention. Changes in the balance and stoichiometry of various nutrients are considered to be one of the most crucial mechanisms for elucidating shifts in phytoplankton communities in coastal ecosystems (Anderson et al., 2002; Liu and Glibert, 2018). The N/P ratio in the BHS has increased markedly from the 1990s to the early 2010s due to the increased reduced nitrogen (NH_4^+-N, terrestrial DON) input into the BHS (Chen et al., 2022). It is generally believed that the shift in the N/P ratio is the main reason for the shift from diatom dominance to a codominance of diatoms and dinoflagellates in the BHS (Luan et al., 2018; Xu et al., 2010). This is because diatoms and dinoflagellates have different survival strategies in response to changes in nutrient structure, that is, dinoflagellates have an advantage over diatoms in high N/P ratios (or phosphorus-limited) environments by hydrolyzing dissolved organic phosphorus (DOP) and producing toxins (Frangópulos et al., 2004; Glibert et al., 2013; Wang et al., 2014).

We observed that the trend in nutrient structure in the BHS during the late summers of 2011–2020 was opposite to that observed from the 1990s to the early 2010s. Specifically, the DIN concentration, N/P ratio, and N/Si ratio showed a downward trend, while the PO_4^{3-}-P concentration showed an upward trend. In particular, since 2016, the N/P ratio in the BHS has approached the Redfield ratio, suggesting that Phosphorus limitation has been alleviated. The EI was significantly higher or lower in specific years, but it did not show an upward or downward trend. According to the division of eutrophication levels, namely: mild eutrophication ($1 \leqslant EI \leqslant 3$), moderate eutrophication ($3 < EI \leqslant 9$), and severe eutrophication ($EI > 9$) (Zhu et al., 2020), the BHS was not eutrophic during the study period. The Chl *a* concentration, which is an important indicator of phytoplankton biomass (Blondeau-Patissier et al., 2014), exhibited a slight downward trend during the study period, completely different from the upward trend during 1998–2018 reported by Tian et al. (2019). Moreover, the Dia/Dino index was found to fluctuate during the study period but did not show an upward or downward trend. The Dia/Dino index in this study was calculated based on abundance data and corresponds to that defined by Wasmund et al. (2017). According to Wasmund et al. (2017), the Dia/Dino index can indicate the marine environmental status and food web changes; a high Dia/Dino index indicates stronger sedimentation and better nutrition of the benthos, while a low Dia/Dino index indicates better nutrition of the pelagic components of the food web. Thus, the trend in the Dia/Dino index suggested that the vertical mass transport and food pathway were generally stable in the BHS during the study period. As trends in the Dia/Dino index vary depending on the sea area and the season (Wasmund et al., 2017), the Dia/Dino index values in this study were compared with the historical data from the BHS in summer. According to the data reported by Luan et al. (2018), after conversion, the summer average Dia/Dino index of the BHS over the past half century (calculated from the averages of the 1960s,

1980s, 1990s, 2000s, and 2010s) is 0.34, with the value for the year 2000 being as low as 0.18. The Dia/Dino index values (0.62–0.94) in our study are generally higher than these historical values, suggesting greater diatom dominance during the study period. Based on the aforementioned indices, the nutrient status in the BHS remained stable during the study period, and the trends of eutrophication, nutrient ratio imbalance, and shifts in phytoplankton community structure observed before the early 2010s did not persist.

We suggest that the N/P ratio, EI, and Dia/Dino index are important indicators that should be taken into account when assessing the ecological status in the BHS. Moreover, studies on the biota in the BHS in summer used to be carried out during June–August; however, the significant intraseasonal variation in the circulation patterns of the BHS could have significantly different impacts on the biota. It is therefore suggested that a comparative study between early summer and late summer in the BHS should be carried out in the future. Additionally, this study specifically examines the trends in community composition and diversity of larger-sized microphytoplankton (>76 μm) and does not address trends in other phytoplankton size classes. Consequently, it is unclear whether the trend of phytoplankton miniaturization in the BHS is ongoing, which also warrants investigation in future studies.

5 Conclusions

In this study, we analyzed the dynamics of the net-collected phytoplankton community structure in the BHS during late summer using microscopic methods. We further explored the connections between these dynamics and environmental changes through correlation analysis. During the late summers of 2011–2020, the N/P ratio in the BHS gradually declined, approaching the Redfield ratio. This indicates a reduction in phosphorus limitation in the BHS. The EI values in the BHS did not display a clear upward or downward trend; instead, they remained low, suggesting that the BHS was not eutrophic during the study period. The Dia/Dino index fluctuated but showed no significant trend, reflecting that the earlier shift from diatom dominance to a codominance of diatoms and dinoflagellates did not persist during this period. The phytoplankton community composition and diversity in the BHS exhibited considerable variations during the late summers of 2011–2020. The species composition, abundance, and diversity were closely linked to both physical factors (i.e., depth, gradient, and temperature) and nutrient factors (i.e., DIN, PO_4^{3-}-P, N/P ratio, and N/Si ratio), while the relative dominance of phyla or the Dia/Dino index was primarily associated with physical factors (i.e., depth and gradient). Interestingly, the relative abundances of diatoms and dinoflagellates exhibited opposite correlations with depth, gradient, temperature, and DO concentration, indicating their different interactions with the environment. Diatoms contributed to an increase in total species number and caused a nonequilibrium abundance distribution among species, whereas dinoflagellates tended to balance the distribution of abundances. Additionally, certain dominant species, such as *Skeletonema costatum* and *Paralia sulcata*, exhibited variations closely related to changes in nutrient structure in the BHS, specifically DIN, DIP, and N/P ratio. Overall, this study elucidates the trend of environmental changes in BHS in recent years and the responses of different phytoplankton groups to these changes. The findings provide insights into the adaptive strategies of coastal ecosystems in response to environmental fluctuations.

References

Alexander H. 2016. Defining the ecological and physiological traits of phytoplankton across marine ecosystem [dissertation]. Cambridge: Massachusetts Institute of Technology

Anderson M P B C, Davies C H, Eriksen R S. 2022. Latitudinal variation, and potential ecological indicator species, in the dinoflagellate genus *Tripos* along 110°E in the south-east Indian Ocean. Deep-Sea Research Part II: Topical Studies in Oceanography, 203: 105150, doi: 10.1016/j.dsr2.2022.105150

Anderson D M, Glibert P M, Burkholder J M. 2002. Harmful algal blooms and eutrophication: nutrient sources, composition, and consequences. Estuaries, 25(4): 704–726, doi: 10.1007/BF02804901

Blanchet F G, Legendre P, Borcard D. 2008. Forward selection of explanatory variables. Ecology, 89(9): 2623–2632, doi: 10.1890/07-0986.1

Blondeau-Patissier D, Gower J F R, Dekker A G, et al. 2014. A review of ocean color remote sensing methods and statistical techniques for the detection, mapping and analysis of phytoplankton blooms in coastal and open oceans. Progress in Oceanography, 123: 123–144, doi: 10.1016/j.pocean.2013.12.008

Burns D A, Mitchell J S. 1982. Further examples of the dinoflagellate genus *Ceratium* from New Zealand coastal waters. New Zealand Journal of Marine and Freshwater Research, 16(1): 57–67

Cao Youhua, Zhu Qiankun. 2021. Study on the intensity and temporal and spatial variation of Yellow Sea Warm Current based on Aqua/MODIS data. Marine Forecasts (in Chinese), 38(6): 93–102

Carstensen J, Andersen J H, Gustafsson B G, et al. 2014. Deoxygenation of the Baltic Sea during the last century. Proceedings of the National Academy of Sciences of the United States of America, 111(15): 5628–5633

Chan A T. 1980. Comparative physiological study of marine diatoms and dinoflagellates in relation to irradiance and cell size. Ⅱ. Relationship between photosynthesis, growth, and carbon/chlorophyll *a* ratio. Journal of Phycology, 16(3): 428–432

Chen Kan, Li Keqiang, Gao Peiyi, et al. 2022. Was dissolved nitrogen regime driving diatom to dinoflagellate shift in the Bohai Sea? Evidences from microcosm experiment and modeling reproduction. Journal of Geophysical Research: Biogeosciences, 127(6): e2021JG006737

Falkowski P G, Woodhead A D. 1992. Primary Productivity and Biogeochemical Cycles in the Sea. New York, NY: Plenum Press

Field C B, Behrenfeld M J, Randerson J T, et al. 1998. Primary production of the biosphere: integrating terrestrial and oceanic components. Science, 281(5374): 237–240, doi: 10.1126/science.281.5374.237

Frangópulos M, Guisande C, deBlas E, et al. 2004. Toxin production and competitive abilities under phosphorus limitation of *Alexandrium* species. Harmful Algae, 3(2): 131–139, doi: 10.1016/S1568-9883(03)00061-1

Ge Ruping, Liu Guangxing, Chen Hongju, et al. 2019. Community characteristics of zooplankton sampled with two plankton nets in Yellow River estuary in spring. Periodical of Ocean University of China (in Chinese), 49(4): 62–70

Gebühr C, Wiltshire K H, Aberle N, et al. 2009. Influence of nutrients, temperature, light and salinity on the occurrence of *Paralia sulcata* at Helgoland Roads, North Sea. Aquatic Biology, 7(3): 185–197

Glibert P M, Kana T M, Brown K. 2013. From limitation to excess: the consequences of substrate excess and stoichiometry for phytoplankton physiology, trophodynamics and biogeochemistry, and the implications for modeling. Journal of Marine Systems, 125: 14–28

Huang Daji, Su Jilan, Backhaus J O. 1999. Modelling the seasonal thermal stratification and baroclinic circulation in the Bohai Sea. Continental Shelf Research, 19(11): 1485–1505, doi: 10.1016/S0278-4343(99)00026-6

Ke Zhixin, Tan Yehui, Ma Yane, et al. 2014. Effects of surface current patterns on spatial variations of phytoplankton community and environmental factors in Sunda shelf. Continental Shelf Re-

search, 82: 119–127, doi: 10.1016/j.csr.2014.04.017
Li Chengxuan, Yang Guipeng, Wang Baodong. 2015. Biological production and spatial variation of dimethylated sulfur compounds and their relation with plankton in the North Yellow Sea. Continental Shelf Research, 102: 19–32, doi: 10.1016/j.csr.2015.04.013
Liu Dongyan, Glibert P M. 2018. Ecophysiological linkage of nitrogen enrichment to heavily silicified diatoms in winter. Marine Ecology Progress Series, 604: 51–63
Liu Changdong, Guo Xiaofeng, Tang Yanli, et al. 2015a. Phytoplankton community composition and its relationship with environmental factors in the artificial reef area around the Qiansan Islets, Haizhou Bay. Journal of Fishery Sciences of China (in Chinese), 22(3): 545–555
Liu Dongyan, Liu Lixue, Di Baoping, et al. 2015b. Paleoenvironmental analyses of surface sediments from the Bohai Sea, China, using diatoms and silicoflagellates. Marine Micropaleontology, 114: 46–54, doi: 10.1016/j.marmicro.2014.11.002
Liu Dongyan, Sun Jun, Chen Zongtao, et al. 2002. Effect of N/P ratio on the growth of a red tide diatom *Skeletonema costatum*. Transactions of Oceanology and Limnology (in Chinese), (2): 39–44
Luan Qingshan, Kang Yuande, Wang Jun. 2018. Long-term changes in the phytoplankton community in the Bohai Sea (1959–2015). Progress in Fishery Sciences (in Chinese), 39(4): 9–18
Luan Qingshan, Kang Yuande, Wang Jun. 2020. Long-term changes within the phytoplankton community in the Yellow Sea (1985–2015). Journal of Fishery Sciences of China (in Chinese), 27(1): 1–11
Margalef R. 1968. Perspectives in Ecological Theory. Chicago: University of Chicago Press
Mokrane Z, Boudjenah M, Belkacem Y, et al. 2019. Report on the diatoms and dinoflagellates distribution along the Algerian coasts: Inter-region comparison. Journal of Resources and Ecology, 10(4): 432–440, doi: 10.5814/j.issn.1674-764x.2019.04.010
Obenour D R, Michalak A M, Zhou Yuntao, et al. 2012. Quantifying the impacts of stratification and nutrient loading on hypoxia in the Northern Gulf of Mexico. Environmental Science & Technology, 46(10): 5489–5496
Pan Huizhu, Li Aifang, Cui Zhengguo, et al. 2020. A comparative study of phytoplankton community structure and biomass determined by HPLC-CHEMTAX and microscopic methods during summer and autumn in the central Bohai Sea, China. Marine Pollution Bulletin, 155: 111172, doi: 10.1016/j.marpolbul.2020.111172
Pielou E C. 1966. The measurement of diversity in different types of biological collections. Journal of Theoretical Biology, 13: 131–144, doi: 10.1016/0022-5193(66)90013-0
R Core Team. 2018. R: A language and environment for statistical computing. Vienna, Austria: R Foundation for Statistical Computing
Raitsos D E, Yi X, Platt T, et al. 2015. Monsoon oscillations regulate fertility of the Red Sea. Geophysical Research Letters, 42: 855–862
Rabalais N N, Cai Weijun, Carstensen J, et al. 2014. Eutrophication-driven deoxygenation in the coastal ocean. Oceanography, 27(1): 172–183, doi: 10.5670/oceanog.2014.21
Rhee G Y. 1982. Effects of environmental factors and their interactions on phytoplankton growth. In: Marshall K C, eds. Advances in Microbial Ecology, vol 6. Boston, MA: Springer, 33–74
Richardson A J, Schoeman D S. 2004. Climate impact on plankton ecosystems in the Northeast Atlantic. Science, 305(5690): 1609–1612
Shannon C E, Weaver W. 1949. The Mathematical Theory of Communication. Urbana, IL: University of Illinois Press, 1–117
Shi Hongyuan, Li Qingjie, Sun Jiacheng, et al. 2020. Variation of Yellow River runoff and its influence on salinity in Laizhou Bay. Journal of Ocean University of China, 19(6): 1235–1244, doi: 10.1007/s11802-020-4413-5
Smayda T J. 2002. Adaptive ecology, growth strategies and the global bloom expansion of dinoflagellates. Journal of Oceanography, 58(2): 281–294, doi: 10.1023/A:1015861725470
Song Nanqi, Wang Nuo, Lu Yue, et al. 2016. Temporal and spatial characteristics of harmful algal blooms in the Bohai Sea during 1952–2014. Continental Shelf Research, 122: 77–84
Straile D. 1997. Gross growth efficiencies of protozoan and metazoan zooplankton and their dependence on food concentration, predator-prey weight ratio, and taxonomic group. Limnology and Oceanography, 42(6): 1375–1385
Sun Deyong, Huan Yu, Wang Shengqiang, et al. 2019a. Remote sensing of spatial and temporal patterns of phytoplankton assemblages in the Bohai Sea, Yellow Sea, and East China Sea. Water Research, 157: 119–133, doi: 10.1016/j.watres.2019.03.081
Sun Jun, Liu Dongyan, Bai Jie, et al. 2004a. Phytoplankton community of the Bohai Sea in winter 2001. Periodical of Ocean University of China (in Chinese), 34(3): 413–422
Sun Jun, Liu Dongyan, Xu Jun, et al. 2004b. The netz-phytoplankton community of the Central Bohai Sea and its adjacent waters in spring 1999. Acta Ecologica Sinica (in Chinese), 24(9): 2003–2016
Sun Jun, Liu Dongyan, Yang Shimin, et al. 2002. The preliminary study on phytoplankton community structure in the central Bohai Sea and the Bohai Strait and its adjacent area. Oceanologia et Limnologia Sinica (in Chinese), 33(5): 461–471
Sun Xuerong, Shen Fang, Brewin R J W, et al. 2019b. Twenty-year variations in satellite-derived chlorophyll-*a* and phytoplankton size in the Bohai Sea and Yellow Sea. Journal of Geophysical Research: Oceans, 124(12): 8887–8912
Tian Hongzhen, Liu Qinping, Goes J I, et al. 2019. Temporal and spatial changes in chlorophyll *a* concentrations in the Bohai Sea in the past two decades. Haiyang Xuebao (in Chinese), 41(8): 131–140
Wang Xiulin, Cui Zhengguo, Guo Quan, et al. 2009. Distribution of nutrients and eutrophication assessment in the Bohai Sea of China. Chinese Journal of Oceanology and Limnology, 27(1): 177–183, doi: 10.1007/s00343-009-0177-x
Wang Dan, Huang Bangqin, Liu Xin, et al. 2014. Seasonal variations of phytoplankton phosphorus stress in the Yellow Sea Cold Water Mass. Acta Oceanologica Sinica, 33(10): 124–135
Wang Yibo, Sun Yanyu, Wang Caixia, et al. 2019a. Net-phytoplankton community structure and its environmental correlations in central Bohai Sea and the Bohai Strait. Aquatic Ecosystem Health & Management, 22(4): 481–493
Wang Baodong, Xin Ming, Wei Qinsheng, et al. 2018. A historical overview of coastal eutrophication in the China Seas. Marine Pollution Bulletin, 136: 394–400, doi: 10.1016/j.marpolbul.2018.09.044
Wang Junjie, Yu Zhigang, Wei Qinsheng, et al. 2019b. Long-term nutrient variations in the Bohai Sea over the past 40 years. Journal of Geophysical Research: Oceans, 124(1): 703–722, doi: 10.1029/2018JC014765
Wasmund N, Kownacka J, Göbel J, et al. 2017. The diatom/dinoflagellate index as an indicator of ecosystem changes in the Baltic Sea 1. Principle and handling instruction. Frontiers in Marine Science, 4: 22
Wei Hao, Zhao Liang, Zhang Haiyan, et al. 2021. Summer hypoxia in Bohai Sea caused by changes in phytoplankton community. Anthropocene Coasts, 4(1): 77–86, doi: 10.1139/anc-2020-0017
Welschmeyer N A. 1994. Fluorometric analysis of chlorophyll *a* in the presence of chlorophyll *b* and pheopigments. Limnology and Oceanography, 39(8): 1985–1992, doi: 10.4319/lo.1994.39.8.1985
Wu Wenfan, Zhai Fangguo, Liu Cong, et al. 2023. Three-dimensional structure of summer circulation in the Bohai Sea and its intraseasonal variability. Ocean Dynamics, 73(11): 679–698, doi: 10.1007/s10236-023-01576-6
Xiao Wupeng, Liu Xin, Irwin A J, et al. 2018. Warming and eutrophication combine to restructure diatoms and dinoflagellates. Water Research, 128: 206–216
Xin Ming, Wang Baodong, Xie Linping, et al. 2019. Long-term changes in nutrient regimes and their ecological effects in the

Bohai Sea, China. Marine Pollution Bulletin, 146: 562–573, doi: 10.1016/j.marpolbul.2019.07.011

Xu Sisi, Song Jinming, Li Xuegang, et al. 2010. Changes in nitrogen and phosphorus and their effects on phytoplankton in the Bohai Sea. Chinese Journal of Oceanology and Limnology, 28(4): 945–952, doi: 10.1007/s00343-010-0005-3

Yu Huaming, Li Ji, Yu Haiqing, et al. 2020. Analysis of the interannual variation of the SST in the Yellow Sea Warm Current area. Marine Forecasts (in Chinese), 37(5): 34–41

Yu Qian, Wang Qing, Yuan Zeyi, et al. 2015. Effects of different phosphorus substrates on growth and phosphatase activity of algae *Paralis sulcata*. Oceanologia et Limnologia Sinica (in Chinese), 46(5): 1018–1023

Yu Junbao, Zhou Di, Yu Miao, et al. 2021. Environmental threats induced heavy ecological burdens on the coastal zone of the Bohai Sea, China. Science of the Total Environment, 765: 142694, doi: 10.1016/j.scitotenv.2020.142694

Zakaria I J, Yanti A, Arbain A, et al. 2016. Study of dinoflagellate species in the waters of Bayur Gulf and Bungus Gulf, Padang City, West Sumatera, Indonesia: Diversity and morphological variations. Asian Journal of Applied Sciences, 4(4): 906–919

Zhai Weidong, Zhao Huade, Zheng Nan, et al. 2012. Coastal acidification in summer bottom oxygen-depleted waters in northwestern-northern Bohai Sea from June to August in 2011. Chinese Science Bulletin, 57(9): 1062–1068, doi: 10.1007/s11434-011-4949-2

Zhou Feng, Huang Daji, Su Jilan. 2009. Numerical simulation of the dual-core structure of the Bohai Sea cold bottom water in summer. Chinese Science Bulletin, 54(23): 4520–4528

Zhou Di, Yu Miao, Yu Junbao, et al. 2021. Impacts of inland pollution input on coastal water quality of the Bohai Sea. Science of the Total Environment, 765: 142691, doi: 10.1016/j.scitotenv.2020.142691

Zhu Zhuoyi, Ng W M, Liu Sumei, et al. 2009. Estuarine phytoplankton dynamics and shift of limiting factors: a study in the Changjiang (Yangtze River) Estuary and adjacent area. Estuarine, Coastal and Shelf Science, 84(3): 393–401

Zhu Genhai, Noman M A, Narale D D, et al. 2020. Evaluation of ecosystem health and potential human health hazards in the Hangzhou Bay and Qiantang Estuary region through multiple assessment approaches. Environmental Pollution, 264: 114791, doi: 10.1016/j.envpol.2020.114791

Supplementary information:

Fig. S1. Distribution of *Skeletonema costatum* in the BHS in the late summers of 2011–2020.

Fig. S2. Distribution of *Paralia sulcata* in the BHS in the late summers of 2011–2020.

Fig. S3. Relationship between the absolute/relative abundances of three phytoplankton phyla (Bacillariophyta, Dinoflagellata, Ochrophyta) and the key environmental factors (a. depth, b. gradient, c. temperature, d. DO, e. Net Ⅰ zooplankton abundance).

Fig. S4. Relationship between the absolute/relative abundances of the dominant genera (*Skeletonema*, *Chaetoceros*, *Pseudo-nitzschia*, *Eucampia*, *Tripos*) and the key environmental factors (a. depth, b. gradient, c. temperature, d. DO, e. Net Ⅰ zooplankton abundance).

Fig. S5. Distribution of *Tripos longipes* in the BHS in the late summers of 2016–2020.

Fig. S6. Heatmap showing the Spearman correlations among environmental factors in the BHS in the late summers of 2011–2020.

Table S1. Information of sampling sites.

Table S2. Selection criteria for sampling layers of environmental factors.

Table S3. List of phytoplankton species recorded in the study.

Table S4. Abundances of phytoplankton taxa and the Dia/Dino index in different regions of the BHS in the late summers of 2011–2020.

Table S5. Statistics of phytoplankton diversity indices in the BHS in the late summers of 2011–2020.

Table S6. Dominant phytoplankton species in the BHS in the late summers of 2011–2020.

The supplementary information is available online at https://doi.org/10.1007/s13131-023-2236-0 and http://www.aosocean.com/. The supplementary information is published as submitted, without typesetting or editing. The responsibility for scientific accuracy and content remains entirely with the authors.